

# Non-Markovian evolution: a quantum walk perspective

N. Pradeep Kumar,<sup>1,\*</sup> Subhashish Banerjee,<sup>2,†</sup> R. Srikanth,<sup>3,‡</sup>

Vinayak Jagadish,<sup>4,5,§</sup> and Francesco Petruccione<sup>4,5,¶</sup>

<sup>1</sup>*The Institute of Mathematical Sciences, C. I. T. Campus, Taramani, Chennai 600113, India*

<sup>2</sup>*Indian Institute of Technology Jodhpur, Jodhpur 342011, India*

<sup>3</sup>*Poornaprajna Institute of Scientific Research, Bangalore- 560 080, India*

<sup>4</sup>*Quantum Research Group, School of Chemistry and Physics,  
University of KwaZulu-Natal, Durban 4001, South Africa*

<sup>5</sup>*National Institute for Theoretical Physics (NITheP), KwaZulu-Natal, South Africa*

Quantum non-Markovianity of a quantum noisy channel is typically identified with information backflow, or, more generally, with departure of the intermediate map from complete positivity. But here, we also indicate certain non-Markovian channels that can't be witnessed by the CP-divisibility criterion. In complex systems, non-Markovianity becomes more involved on account of subsystem dynamics. Here we study various facets of non-Markovian evolution, in the context of coined quantum walks, with particular stress on disambiguating the internal vs. environmental contributions to non-Markovian backflow. For the above problem of disambiguation, we present a general power-spectral technique based on a distinguishability measure such as trace-distance or correlation measure such as mutual information. We also study various facets of quantum correlations in the transition from quantum to classical random walks, under the considered non-Markovian noise models. The potential for the application of this analysis to the quantum statistical dynamics of complex systems is indicated.

PACS numbers: 03.65.Ud, 03.67.-a

---

\* pradeepnpk@imsc.res.in

† subhashish@iitj.ac.in

‡ srik@poornaprajna.org

§ JagadishV@ukzn.ac.za

¶ petruccione@ukzn.ac.za

## I. INTRODUCTION

The interaction between quantum system and various subsystems is inevitable for achieving complex quantum information processing tasks. The subsystems could either be some uncontrollable environment that leads to dissipation and decoherence [1–5] or it could be used to implement sophisticated techniques such as reservoir engineering, which enhances the stability of peripheral tasks such as quantum state preparation and readout in quantum computers [6–9]. While the study of open system dynamics presumes an environment that is largely inaccessible, a greater understanding of the influence of the environment on the system dynamics is indispensable for the advancement of quantum technologies.

A huge body of works on open system dynamics has concentrated on the Markovian approximation, where the environmental time-scales are much shorter than the system time-scales [10, 11]. However, current advancement in experimental techniques allows for the possibility of going beyond the standard Markovian regime into non-Markovian regime where the reservoir effectuates memory effects in the system dynamics.

In particular, an example of a non-Markovian experimental realization would be [12–14], a nanomechanical oscillator interacting with a BEC in a double-well potential. The atoms of the condensate are confined in a double well and can tunnel from one side of the potential to the other, depending on the position of the oscillator. If the condensate is taken to be the environment for the oscillator, highly non-Markovian effects appear that can be observed in the non-exponential decay of the oscillator coherences [15, 16]. In a recent experiment [17] it was shown that the spectral density of the environment in Quantum Brownian motion (see below) in an optomechanical resonator coupled to a heat bath, is highly non-Ohmic and produces non-Markovian dynamics in the resonator.

Quantum Brownian motion is a paradigm model of quantum statistical mechanics and has provided a fertile ground for studies related to non-Markovian phenomena, antedating the corresponding developments in quantum information [18–21].

From a quantum information theoretic perspective, non-Markovianity is now usually defined by the condition of information backflow, by which is meant the increase of distinguishability with time between any two given states, as witnessed by measures like trace distance [22–24]; or by the weaker condition of CP-divisibility, by which is meant that the time-evolution generated by the dynamical maps cannot be divided into intermediate maps that are completely positive

(CP-Divisibility) [10, 25]. It is known that for invertible maps, these two conditions are equivalent.

In general not all given dynamics strictly satisfy both the above conditions for it to be termed non-Markovian [26]. CP divisibility is known to imply a lack of information backflow, with the converse also holding true for invertible maps. Though efforts towards connecting the divisibility and information flow pictures has been undertaken in [26, 28], the general conditions under which both these methods coincide for any given non-Markovian dynamics is still an open question. In [27], it is shown that even if the map is non-invertible, lack of information backflow implies a completely positive propagator, which may, however not be trace preserving.

In this work, we wish to demonstrate the occurrence of backflow in a discrete-time quantum walk (DTQW) system, the quantum analogue of “classical random walk” (CRW). Quantum walk is a ubiquitous platform for studying diverse features such as symmetries, quantum to classical transition [3]. The simplest instance of DTQW is that of a quantum system with two levels translating on a one dimensional discrete position space [29, 30], a topology which we use in this work. What makes DTQW especially interesting is that even in the noiseless case, the reduced dynamics of the coin manifests non-Markovian recurrence behavior due to interaction with the position degree of freedom [31]. This could be also envisaged in more complex systems which may possess an inherent non-Markovian feature because of interaction among subsystems. In [32], a method was proposed to disambiguate this internal source from environmental non-Markovianity, whose applicability would extend beyond the model chosen here. The various noisy channels we consider are a local dephasing non-Markovian noise model [33] modeled on the random telegraph noise (RTN) process [34], the modified Ornstein-Uhlenbeck (OU) [35, 36] and the power law noise (PLN) [37]. Backflow can also be witnessed by the revival of various facets of quantum correlations in the transition from quantum to classical [38] random walks, under the considered non-Markovian noise models.

We begin with a brief description of the DTQW as well as the different non-Markovian noise models used in this work. This is followed by a study of the variance of the quantum walk (QW), evolving under the influence of different noises. Signatures of non-Markovianity are probed next by making use of trace distance and mutual information. This is followed by a discussion of the recently developed power spectrum method [32] to disambiguate the different sources of non-Markovianity. The recurring theme of this work, i.e., to develop insights into the non Markovian behavior is further developed by studying various facets of quantum correlations between the coin and position states of the DTQW. We then make our conclusions.

## II. BRIEF INTRODUCTION TO DTQW AND NON-MARKOVIAN NOISE MODELS

### A. DTQW: A brief introduction

The formalism of DTQW requires two essential ingredients, the *coin* and the *walker* [39], which describes the internal and external degrees of freedom of the particle, respectively. The coin degree of freedom is spanned by the basis set  $\{|0\rangle, |1\rangle\} \in \mathcal{H}_c$  and the walker or position translational degree of freedom is spanned by the basis  $\{|i\rangle\} \in \mathcal{H}_p$  with  $i \in \mathbb{Z}$  representing the number of lattice sites available to the walker. The state of total system is described by the Hilbert space  $\mathcal{H}_w = \mathcal{H}_c \otimes \mathcal{H}_p$ .

To implement the DTQW, we initialize a quantum state  $|\psi(0)\rangle$  specified by two parameters  $\delta, \eta$ ,

$$|\psi(\delta, \eta)\rangle = (\cos(\delta)|0\rangle + e^{-i\eta}\sin(\delta)|1\rangle)|x\rangle \quad (1)$$

where  $x \in \{-n, -(n-1), \dots, 0, 1, \dots, n\}$ , and the first register refers to the coin degree of freedom, which lives in the two-dimensional Hilbert space  $\mathcal{H}_C$ , and the second register refers to the position degree of freedom, which lives in the  $(2n+1)$ -dimensional Hilbert space  $\mathcal{H}_P$ . Here, we shall set the initial walker state  $|\psi(t=0)\rangle$  to be  $|\psi(\delta = \frac{\pi}{4}, \eta = 0)\rangle |x = 0\rangle$ .

The quantum walker is then evolved using the coin and shift (position translation) operators. The action of coin operator determines the direction in which the particle moves. The general form of coin operator is that of a rotation matrix  $U(2)$ , in two dimensional Hilbert space, given by

$$\hat{C} = \begin{bmatrix} \cos \theta_c & \sin \theta_c \\ \sin \theta_c & -\cos \theta_c \end{bmatrix}. \quad (2)$$

For  $\theta_c = 45^\circ$ ,  $\hat{C}$  reduces to Hadamard operator, the quantum walk with such a coin is also called Hadamard quantum walk [29].

The shift operator that translates the particle to either left or right is conditioned on the outcome of the coin operator. The general form of the shift operator is given as,

$$\hat{S} = |0\rangle\langle 0| \otimes \sum_{x \in \mathbb{Z}} |x-1\rangle\langle x| + |1\rangle\langle 1| \otimes \sum_{x \in \mathbb{Z}} |x+1\rangle\langle x|. \quad (3)$$

The combination of both the coin and shift operators, denoted  $W \equiv \hat{S}(\hat{C} \otimes \mathbb{I}_P)$ , represents the walk operator on the total Hilbert space. Consequently, the quantum state of the particle after  $t$  steps of noiseless quantum walk is the linear superposition of  $2t+1$  position states,

$$|\psi(t)\rangle = \hat{W}^t |\psi(0)\rangle \quad (4)$$

where  $W^t$  denotes applying the walk operator ( $W$ )  $t$  times. The noisy case is handled numerically, in the conventional way, by applying an instance of the noise super-operator  $\mathcal{E}_t \equiv \mathcal{E}(t+1, t)$  (realized by the Kraus operators  $K_j(t+1 : t)$  after each application of the  $W$  operation [2, 3, 40], where the Kraus operators must correspond to the intermediate map (time evolution from  $t$  to  $t+1$ ). In this case, Eq. (??) is replaced by:

$$\rho(t) = \left[ \Pi_t(\mathcal{E}_t \mathcal{W}) \right] (\rho(0)) \quad (5)$$

where  $\rho(0) \equiv |\psi(0)\rangle \langle \psi(0)|$  and  $\mathcal{W}$  is the walk superoperator corresponding to  $W$  (i.e, the action  $W\rho W^\dagger$ ) i.e., action of unitary  $W$  on a density operator  $\rho$ , while  $\Pi_t$  is the product of the time sequence of operations:  $(\mathcal{E}_t \mathcal{W})(\mathcal{E}_{t-1} \mathcal{W}) \dots (\mathcal{E}_1 \mathcal{W})$ .

With non-Markovian noise, especial care is needed, since the intermediate map could be a non-completely positive (NCP). Importantly, the backflow element of RTN, to be studied below, means that this map may cause the Kraus operator-sum representation to be replaced by an operator-sum-difference representation, a detailed discussion of this will appear in section III. In this present work, we adopt a simpler approach, where the Kraus operators  $K_j(0; t)$  are applied once after  $t$  QW steps [32]. One expects this to qualitatively reproduce the significant features that would be obtained under the application of the intermediate map at each step. We discuss elsewhere the difference between these two methods.

## B. Non-Markovian Noise

Here we briefly discuss, from the perspective of their stochastic properties, local non-Markovian dephasing noise, due to the environment, which will be subsequently acted on the coin degrees of freedom of the quantum walker.

### 1. Random Telegraph Noise

We now discuss a local non-Markovian dephasing noise, studied in [33] and motivated by the Random Telegraph Noise (RTN) [34]. The effect of RTN on the dynamics of quantum systems, specifically quantum correlations such as quantum discord has been studied extensively in [41–43]. RTN was also studied in the context of control of open system dynamics [44].

The autocorrelation function for the RTN, represented by the stochastic variable  $\Upsilon(t)$ , is given by,

$$\langle \Upsilon(t) \Upsilon(s) \rangle = a^2 e^{-|t-s|\gamma}, \quad (6)$$

where  $a$  has the significance of the strength of the system-environment coupling and  $\gamma$  is proportional to the fluctuation rate of the RTN. The corresponding power spectral density is a Lorentzian with peak value given by  $2a^2/\gamma$ . The Kraus operators, representing the RTN dynamical map are given by,

$$\begin{aligned} K_1(t) &= \sqrt{\frac{1+\Lambda(t)}{2}} I, \\ K_2(t) &= \sqrt{\frac{1-\Lambda(t)}{2}} \sigma_3, \end{aligned} \quad (7)$$

satisfying the completeness relation  $\sum_{n=1}^2 K_n^\dagger K_n = I$ .  $\Lambda(t)$  is the noise function based on the damped harmonic oscillator model that encompasses both the Markovian and non-Markovian limits of the noise acting on the qubit,

$$\Lambda(t) = e^{-\gamma t} \left[ \cos \left( \left[ \sqrt{\left(\frac{2a}{\gamma}\right)^2 - 1} \right] \gamma t \right) + \frac{\sin \left( \left[ \sqrt{\left(\frac{2a}{\gamma}\right)^2 - 1} \right] \gamma t \right)}{\sqrt{\left(\frac{2a}{\gamma}\right)^2 - 1}} \right], \quad (8)$$

where  $\sqrt{\left(\frac{2a}{\gamma}\right)^2 - 1}$  is the frequency of the harmonic oscillators. A power series expansion of  $\Lambda(t)$  indicates the absence of the term linear in  $t$  bringing about a fundamental difference between white noise and colored noise. The function  $\Lambda(t)$  corresponds to two regimes; the purely damping regime, where  $a/\gamma < 0.25$ , and damped oscillations for  $a/\gamma > 0.25$ . Corresponding to these two regimes of  $\Lambda(t)$ , we observe Markovian and non-Markovian behavior, respectively, both according to the CP-divisibility (Fig. (2)) and backflow criteria (Sec. (4 and 5)).

## 2. Modified Ornstein-Uhlenbeck and Power law Noises

Here, we briefly introduce the modified Ornstein-Uhlenbeck and Power law noises, which, as we will see, have similar structures. The modified Ornstein-Uhlenbeck noise, from now on referred to as OUN, is a well known stationary Gaussian random process which is in general a non-Markovian process but possess a well defined Markov limit [35]. An example of a physical scenario that leads to the OUN is when the spin of an electron interacts with a magnetic field subject to stochastic fluctuations.

Power law noise (PLN), also called  $1/f^\alpha$  noise is a non-Markovian stationary noise process, where  $\alpha$  is some real number. The name ‘Power Law’ is attributed to the functional relationship between the spectral density and the frequency of the noise. The PLN is a major source of decoherence in solid state quantum information processing devices such as superconducting qubits

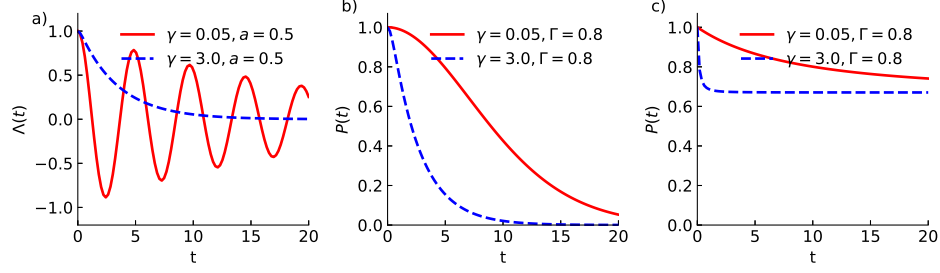


FIG. 1. (Color online) Plot of the noise functions that appear in the noise models. Note that the blue dashed line represents the Markovian regime while the red solid line corresponds to the non-Markovian regime. (a) RTN: The damped oscillations curve corresponds to the non-Markovian regime of the noise while the exponential decay curve is the typical Markovian regime (b) OUN: Unlike RTN, the non-Markovian regime of OUN does not show damped oscillations. Instead, it has a power law behaviour which in contrast to the exponential decay observed in the Markovian regime. PLN: Similar to OUN,  $P(t)$  decays without any oscillations.

[45]. PLN, like OUN, is in general a non-Markovian process but possess a well defined Markovian limit.

The autocorrelation functions for OUN and PLN, represented by the stochastic variable  $\Omega(t)$ , are

$$\langle \Omega(t)\Omega(s) \rangle = \begin{cases} \Gamma\gamma e^{-\gamma|t-s|}, & \text{OUN} \\ \frac{1}{2}(\alpha - 1)\alpha\Gamma \frac{1}{(\gamma|t-s|+1)^\alpha}. & \text{PLN} \end{cases} \quad (9)$$

The spectral properties of the noises are given by  $\gamma$ , which specifies the noise bandwidth and  $\gamma^{-1} = \tau_c$  is the finite correlation time of the environment. The parameter  $\Gamma$  is the effective relaxation time which is an experimentally determinable quantity, often referred to as  $T_1$  time in the literature.

The dynamical map corresponding to the system density matrix can be expressed in terms of the Kraus operators as [36]

$$\begin{aligned} K_1(t) &= \sqrt{\frac{1+P(t)}{2}} I, \\ K_2(t) &= \sqrt{\frac{1-P(t)}{2}} \sigma_3, \end{aligned} \quad (10)$$

where

$$P(t) = \begin{cases} \exp[-\frac{\Gamma}{2}(t + \frac{1}{\gamma}(e^{-\gamma t} - 1))], & \text{OUN} \\ \exp(-\frac{t(t\gamma+2)\Gamma\gamma}{2(t\gamma+1)^2}) & \text{PLN.} \end{cases} \quad (11)$$

All the parameters have the same meaning as above.

For the OUN scenario, for sufficiently large values of the noise bandwidth,  $\gamma \rightarrow \infty$ , the correlation time  $\tau_c \rightarrow 0$  and hence the correlation function becomes  $\langle \Omega(t)\Omega(s) \rangle \rightarrow \Gamma\delta(t-s)$ , whence the Markov property of the OUN is obtained. In this limit, the coherence terms decay exponentially as  $P(t) \rightarrow e^{-\Gamma t}$ . On the other hand, when  $\gamma$  is finite, the resulting spectrum is Lorentzian as opposed to the delta function in the Markovian regime. Here, the decay rate slows down to a polynomial value of  $P(t) \rightarrow 1 - \frac{1}{2}\Gamma\gamma t^2$  (in the limit  $\gamma \approx 0$ ). In Fig. 1, different regimes of all the noise sources considered are explicitly shown.

### III. INTERMEDIATE MAPS AND COMPLETE POSITIVITY:

Two major (often inequivalent) criteria for witnessing non-Markovian behavior are information backflow [22, 23] and departure from CP-divisibility of the intermediate map connecting the density operators  $\rho(t_2)$  and  $\rho(t_1)$  at times  $t_2$  and  $t_1$ , with  $t_2 > t_1$  [10, 25]. Both methods are discussed here and found to be equivalent for the noise models considered.

Given a dynamical map  $\mathcal{E}(t_2, t_0)$  linking a system's density operator at times  $t_0$  and  $t_2 > t_0$ , the intermediate map  $\mathcal{E}^{\text{IM}}(t_2, t_1)$  for some intermediate time  $t_1$  such that  $t_2 > t_1 > t_0$ , is given by:

$$\mathcal{E}^{\text{IM}}(t_2, t_1) = \mathcal{E}(t_2, t_0)\mathcal{E}^{-1}(t_1, t_0). \quad (12)$$

provided that the inverse map  $\mathcal{E}^{-1}(t_1, t_0)$  exists. The Choi matrix for the intermediate map can be obtained as:

$$M_{\text{choi}} = (\mathcal{E}^{\text{IM}}(t_2, t_1) \otimes \mathbb{1}) |\Phi^+\rangle \langle \Phi^+|, \quad (13)$$

where  $|\Phi^+\rangle \equiv |00\rangle + |11\rangle$ . In the following subsections, following the method presented in [10], we briefly derive the intermediate dynamical maps of the noisy channels RTN, OUN and PLN.



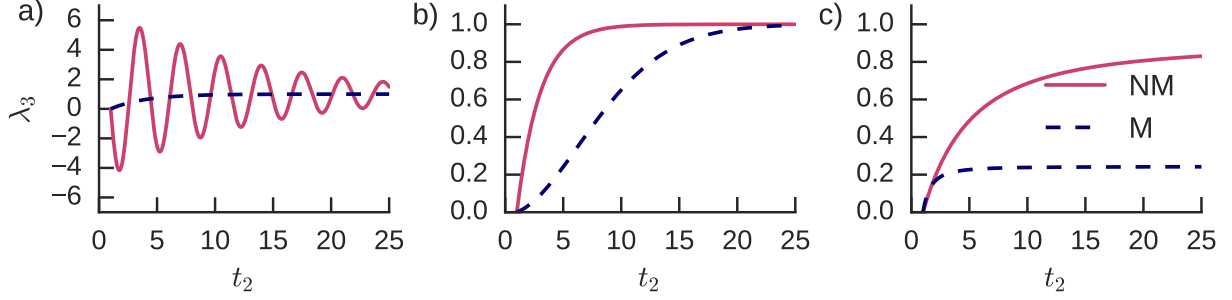


FIG. 2. (Color online) The eigenvalue  $\lambda_3$  of the Choi matrix obtained from intermediate dynamical map in both the Markovian and non-Markovian for different noise models (see Eqs. (??) and (??)). The initial time  $t_1 = 1$  is fixed for all the plots (a) RTN: In the non-Markovian regime ( $\gamma = 0.05, a = 0.9$ ) we observe  $\lambda_3$  oscillating between positive and negative eigenvalues and in the Markovian regime ( $\gamma = 5, a = 0.9$ )  $\lambda_3$  is always positive. (b) OUN: In both the non-Markovian ( $\gamma = 0.05, \Gamma = 1.0$ ) and the Markovian regime ( $\gamma = 5.0, \Gamma = 1.0$ )  $\lambda_3$  is positive. (c) PLN: Similar to OUN, no negative value for  $\lambda_3$  is observed in both the non-Markovian regime ( $\gamma = 0.05, \Gamma = 5.0$ ), Markovian regime ( $\gamma = 2.0, \Gamma = 5.0$ ).

### A. Intermediate map for RTN

The Choi matrix corresponding to the intermediate map for RTN is found to be,

$$M_{\text{choi}} = \begin{bmatrix} 1 & 0 & 0 & \frac{\Lambda(t_2)}{\Lambda(t_1)} \\ 0 & 0 & 0 & 0 \\ 0 & 0 & 0 & 0 \\ \frac{\Lambda(t_2)}{\Lambda(t_1)} & 0 & 0 & 1 \end{bmatrix}. \quad (14)$$

The non-vanishing eigenvalues of  $M_{\text{choi}}$  in Eq. (14) are,

$$\lambda_3 = \left[ 1 - \frac{\Lambda(t_2)}{\Lambda(t_1)} \right]; \lambda_4 = \left[ 1 + \frac{\Lambda(t_2)}{\Lambda(t_1)} \right]. \quad (15)$$

Here  $\lambda_1$  and  $\lambda_2$  are the vanishing eigenvalues. It may be checked that if  $2a \ll \gamma$ , then  $\Lambda(t)$  is a monotonically decreasing function and all eigenvalues are positive at all times (Fig. 2. a), consistent with the Markovian limit of RTN. On the other hand, if  $2a \gg \gamma$ , then  $\Lambda(t)$  can have regions of increase, and correspondingly, some eigenvalues can be negative (Fig. 2.a), consistent with the non-Markovian regime limit of the dynamical map.

Generalizing the Choi method [46, 47] to possibly NCP maps, the Kraus operators for the intermediate map are obtained by “folding” the above eigenvectors [48]

$$K_{\pm}^{\text{IM}} = \sqrt{\frac{1}{2} \left| 1 \pm \frac{\Lambda(t_2)}{\Lambda(t_1)} \right|} \begin{pmatrix} 1 & 0 \\ 0 & \pm 1 \end{pmatrix}. \quad (16)$$

Note that if all eigenvalues are positive, then these Kraus operators satisfy the completeness condition  $K_+^{\text{IM}\dagger}K_+^{\text{IM}} + K_-^{\text{IM}\dagger}K_-^{\text{IM}} = \mathbb{1}$  and the evolution has the operator-sum form:  $\rho \longrightarrow \sum_j K_j^{\text{IM}}\rho K_j^{\text{IM}\dagger}$ . This characterizes the situation in the Markovian regime.

But if some eigenvalues are negative (in fact,  $\lambda_3$ ), then observe that because of the way the absolute value is taken in defining the Kraus operators, these operators satisfy the completeness condition with a minus sign. Quite generally, we have completeness of the type

$$K_-^{\text{IM}\dagger}(t_1, t_2)K_-^{\text{IM}}(t_1, t_2) \pm K_+^{\text{IM}\dagger}(t_1, t_2)K_+^{\text{IM}}(t_1, t_2) = \mathbb{1}, \quad (17)$$

where the sign  $\pm$  is determined by whether or not  $\lambda_3$  is negative. Correspondingly, the evolution has the operator-sum or operator-sum-difference form [49]:

$$\begin{aligned} \rho &\longrightarrow K_-^{\text{IM}}(t_1, t_2)\rho K_-^{\text{IM}\dagger}(t_1, t_2) \pm K_+^{\text{IM}}(t_1, t_2)\rho K_+^{\text{IM}\dagger}(t_1, t_2) \\ &\equiv \mathcal{E}(t_1, t_2)[\rho]. \end{aligned} \quad (18)$$

This characterizes the general situation, no matter whether the evolution is Markovian or non-Markovian.

### B. Intermediate map for OUN and PLN

Following the recipe (13), the Choi matrix for OUN is obtained as

$$M_{\text{choi}} = \begin{bmatrix} 1 & 0 & 0 & \frac{p(t_2)}{p(t_1)} \\ 0 & 0 & 0 & 0 \\ 0 & 0 & 0 & 0 \\ \frac{p(t_2)}{p(t_1)} & 0 & 0 & 1 \end{bmatrix}, \quad (19)$$

for which the eigenvalues are,

$$\lambda_1 = \lambda_2 = 0; \lambda_3 = \left[1 - \frac{p(t_2)}{p(t_1)}\right]; \lambda_4 = \left[1 + \frac{p(t_2)}{p(t_1)}\right], \quad (20)$$

with the intermediate map Kraus operators given by:

$$K_{\pm}^{\text{IM}} = \sqrt{\frac{1}{2} \left| 1 \pm \frac{p(t_2)}{p(t_1)} \right|} \begin{pmatrix} 1 & 0 \\ 0 & \pm 1 \end{pmatrix}. \quad (21)$$

The parameter  $p(t)$  for the OUN and PLN noises can be seen from (??). It is evident from the form of the probability  $p(t)$ , that this function is monotonically decreasing and hence these eigenvalues

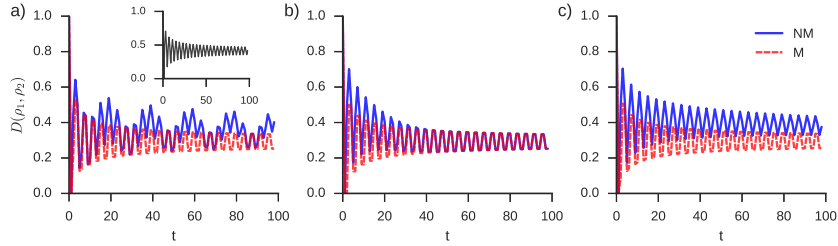


FIG. 3. (Color online) Plot of TD evolution with respect to number of time steps  $t$ , for the initial states  $|\psi(\pm\frac{\pi}{4}, 0)\rangle$  under the influence of different non-Markovian noise sources. The curves in the plot indicate the noiseless quantum walk (inset plot), the Markovian regime (red dashed line) and non-Markovian regime (blue solid line) of the respective noise sources. (a) RTN: The noiseless quantum walk, i.e., the QW in the absence of an external noise, shows rapid recurrences due to interaction with the position “environment”, while the non-Markovian regime ( $\gamma = 0.001, a = 0.08$ ) shows an additional oscillatory term attributed to the non-Markovianity in the environment-induced decoherence, which is absent in the Markovian regime ( $\gamma = 7.0, a = 1.0$ ). (b) OUN: In the Non-Markovian regime ( $\gamma = 0.01, \Gamma = 0.1$ ), TD decays without the additional recurrent feature seen in the RTN case. (c) PLN is similar to OUN in this respect. Noise parameters are same as OUN

are never negative. Therefore, even in the non-Markovian regime, the intermediate map remains CP. Later, we shall find that, similarly, no backflow features show up in this case.

Below, we shall consider non-Markovianity indicated by the distinguishability criterion applied to the reduced dynamics of the coin in a DTQW, subjected to the above three noise models.

#### IV. SIGNATURES OF NON-MARKOVIANITY

It is evident from the above discussions that non-Markovian behavior is capable of throwing a number of surprises. Hence it becomes imperative to have means by which this behavior can be studied quantitatively. In what follows, we will attempt this using two well known measures, trace distance (TD) between two initial states, and coin-position mutual information (MI) to study non-Markovian backflow behavior under QW evolution.

##### A. Trace distance

As mentioned before, a powerful diagnostic of non-Markovian character, encoded in the dynamics of quantum systems, is the backflow of information from the environment to the system. This, in turn manifests in the form of oscillations in correlation measures such as quantum mutual in-

formation [50], and trace distance [51], which are otherwise monotonic functions if the dynamics is Markovian. The distance between any two quantum states defined on the space of density matrices is given by a metric called the TD. It is defined as

$$D(\rho_1, \rho_2) = \frac{1}{2} \text{Tr} \|\rho_1 - \rho_2\|, \quad (22)$$

where  $\|A\|$  is the operator norm given by  $\sqrt{A^\dagger A}$ . TD encompasses the idea of distinguishability of a pair of quantum states, which is monotonically decreasing under completely positive (CP) maps  $\Xi$ , *i.e.*, the CP maps are contractions for this metric,

$$D(\Xi \rho_1, \Xi \rho_2) \leq D(\rho_1, \rho_2). \quad (23)$$

For non-Markovian processes, due to the backflow of information from the environment to the system, there is a temporary increase in the distinguishability of quantum states and hence the above inequality may be violated (this being the characteristic of backflow). This idea has been exploited in an effort to quantify non-Markovianity [22].

Initially, we consider the noiseless (unitary) evolution of the quantum walk. To study the reduced dynamics of the coin state, we initialize the quantum states,  $|\pm\rangle = \frac{|0\rangle \pm |1\rangle}{\sqrt{2}}$ , and compute TD between the two states defined above using Eq. (22). Since the evolution is governed by unitary dynamics the overall evolution of the quantum walk remains unitary and hence the TD is preserved. However, TD measure between the reduced coin states undergo high frequency oscillation as shown in Fig. 3. Such TD oscillations are a signature of non-Markovian backflow behavior leading to non-zero value of the non-Markovian measures [31]. In addition to the oscillations present in the noiseless evolution of quantum walk, a further oscillatory or recurrence structure arises when the coin is exposed to an external noise such as RTN in the non-Markovian regime, as depicted in Fig. 3.(a). We also observe that unlike RTN, neither OUN nor PLN causes new recurrences. Instead, non-Markovianity manifests by way of the trace distance between the two coin states diminishing more slowly as compared to their Markovian counterpart, as shown in Figs. 3.(b) and (c), respectively.

## B. Mutual Information

Quantum correlations has been used to understand non-Markovianity in dynamical maps. In particular, MI has been used to quantify non-Markovianity [50]. Let  $\rho_1$  and  $\rho_2$  be the density matrices representing the system and the ancillary states, respectively. The quantum correlation

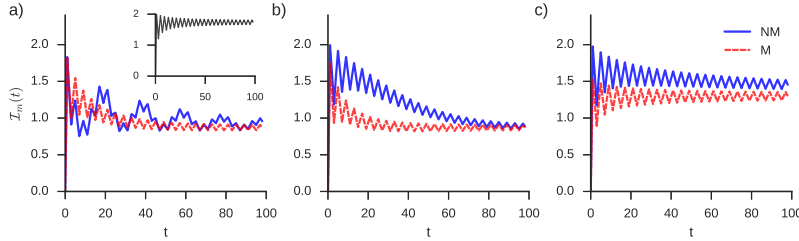


FIG. 4. (Color online) Plot of MI evolution with respect to number of time steps  $t$ ,  $|\psi(\pm\frac{\pi}{4}, 0)\rangle$ , under the influence of different non-Markovian noise sources. The curves in the plot indicate the noiseless quantum walk (inset), the Markovian regime (red dashed line) and non-Markovian regime (blue solid line) of the respective noise sources. (a) RTN: Oscillations are observed in the noiseless quantum walk, similar to TD, arising from the position environment. In the non-Markovian regime ( $\gamma = 0.01, a = 0.08$ ), the information backflow arising in the form of oscillations shortly after a few initial time steps is observed. (b) OUN: In the Non-Markovian regime ( $\gamma = 0.01, \Gamma = 0.5$ ), MI decays without any recurrences from the environment, indicating the absence of the backflow feature which manifests in the RTN case. However the correlation is preserved in the non-Markovian regime for longer time steps. (c) PLN is similar to OUN but preserves the correlation for a longer time in both the regimes. Noise parameters are same as OUN

between the  $\rho_1$  and  $\rho_2$  is given by,

$$\mathcal{I}(\rho) = S(\rho_1) + S(\rho_2) - S(\rho), \quad (24)$$

where  $S(\cdot)$  is the Von Neumann entropy  $S(\rho_1) := -\text{Tr}\rho_1 \log_2 \rho_1$ . Similar to the TD measure, MI is also a monotonically decreasing function when the dynamics is Markovian,

$$\mathcal{I}((\Xi \otimes \mathbb{I})\rho) \leq \mathcal{I}(\rho), \quad (25)$$

leading to a measure of non-Markovianity based on MI. The quantum correlation between the coin and the position can be quantified using MI. This in turn could serve as a method to detect non-Markovianity in the quantum walk evolution. Similar to TD oscillation seen in the noiseless quantum walk, MI also encodes the same features, as shown in Fig. 4. Similar to the variance of the QW, MI is useful for demonstrating the quantum to classical transition. When the coin is driven by a noise, irrespective of its characteristics, MI tend to vanish in the long time limit. However, it is the short time behavior that is of interest to us here. In Figs. 4.(a-c), are depicted the results of the short time behavior of MI under different noise models. In the case of RTN, due to the presence of backflow of information, MI revives periodically, as shown in Fig. 4(a). In the case of OUN and PLN, non-Markovianity manifests by way of preservation of the correlation for a longer period of time compared to the Markovian regime, as shown in Fig. 4(b). Now we discuss a

method to disambiguate different sources of non-Markovianity. This is natural to the QW system, studied here, but could be also be envisaged in more complex systems, such as the suppression of decoherence due to two competing sources leading to frustration, a feature of use in fault tolerant holonomic quantum computation [52, 53].

## V. DISAMBIGUATING DIFFERENT SOURCES OF NON-MARKOVIANITY

The study of both TD and MI in the previous section, clearly shows how non-Markovianity originates from both the subsystem dynamics such as position and purely from environmental sources like RTN. In such a scenario, identifying the different sources of non-Markovianity would be useful in comparing the relative strengths of different sources with respect to one another. Here, we employ a recently developed [32] time domain filtering and power spectral method to disambiguate the position non-Markovianity from environment induced non-Markovianity. Our method is grounded on the observation that, different sources of non-Markovianity induce different frequencies of oscillation in the time evolution of either TD or MI or any other similar correlation measure. By applying a proper filtering function to TD or MI we can detect the frequencies of the oscillation induced by both position and environmental noise. Fig. 5.(c) is the actual power spectrum of TD between two coin states driven by RTN and Fig. 5.(d) is the filtered power spectrum obtained by subtracting the TD curve from its corresponding Monotonically Falling Best Fit Function (MFBF).

The MFBF is simply a best fit function subject to the condition of strictly monotonic decrease. The form of the function is guided by the form of the function in the corresponding Markovian limit. The basic rationale behind this approach is that with high probability, different sources of backflow (e.g., the environment and another subsystem, such as the coin or position) correspond typically to different recurrence time-scales overlaid on an underlying Markovian trend. This trend can be filtered out as a low frequency component, whereas the various backflow contributions can be separated in the Fourier domain as different frequency components. We stress that subtracting the Markovian trend as the MFBF is a heuristic principle to pre-process the data before Fourier analysis. Future work can evolve more finely tuned ways to implement this idea.

The most general recipe for identifying the MFBF can be cast as a monotone regression problem, in which the best fit function can be obtained using constrained optimization techniques. For example, minimizing non-linear least squares subjected to strict monotone decreasing condition

amounts to solving a quadratic optimization problem [54],

$$\text{minimize } \sum_{i=1}^n w_i (g(x_i) - f(x_i))^2 \quad (26)$$

$$\text{subject to } x_{i+1} - x_i < 0, \quad (27)$$

where  $g(x_i)$ ,  $i = 1, \dots, n$ , is the best fit function subjected to condition (27),  $f(x_i)$ ,  $i = 1, \dots, n$ , is the given function and  $w_i$ ,  $i = 1, \dots, n$ , is the appropriate weight.

The filtered spectrum, as shown is obtained by fitting an exponential curve which serves as the MFBF, which when subtracted from the actual TD curve clearly detects the presence of both position and environment induced non-Markovianity. In Fig. 5.(c) the peak around  $f = 0.27$  (resp.  $f = 0.025$ ) corresponds to the position (resp., RTN) non-Markovian source, with the power associated with the former about 1.5 times more. The key point here is that in the RTN case, information backflow to the system from the position or RTN reservoirs, show up as separate peak frequencies in the power spectrum of Fig. 5.(d). However, for the OU noise, we find that information backflow, indicated by the secondary peak in the filtered power spectrum, is absent. Here, the reservoir has a low bandwidth,  $\gamma$ , resulting in a large reservoir correlation time in relation to the system correlation time.

## VI. QUANTUMNESS OF QUANTUM WALK

The time evolution of quantum walk induces non-classical correlations between coin and position degrees of freedom. The usual signature of quantum walk is the quadratic growth in variance, in contrast to the classical random walk for which it is linear in time [29]. Other than studying variance, greater insight into the non-Markovian nature of the QW due to the coin-position nonclassical correlations can be developed by studying correlation measures, such as measurement-induced disturbance (MID) and Quantum Discord (QD) [55, 56]. In addition, we find that the quantum state purity can be a useful diagnostic here, in the sense that it indicates the effect of entanglement with environment.

### A. Measurement Induced Disturbance

To evaluate MID over the QW evolution, we consider a state  $\rho$  evolving in the Hilbert space  $\mathcal{H}_c \otimes \mathcal{H}_p$  and the corresponding reduced density matrices represented by  $\rho_c$  and  $\rho_p$ . Let the projectors  $\{\Pi_n\}$  denote the measurement operators, satisfying the usual properties such as completeness

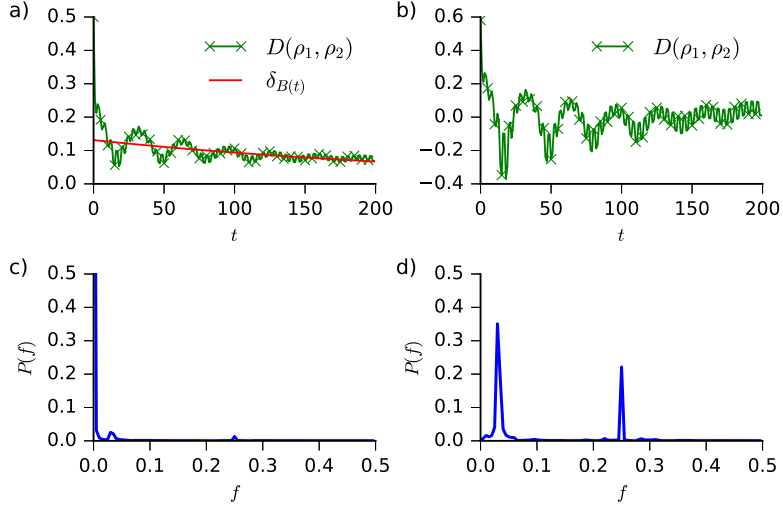


FIG. 5. (Color online) Filtering and power spectral analysis of TD between coin states  $|\psi(\pm\frac{\pi}{4}, \frac{\pi}{3})\rangle$  driven by RTN. (a) Plot of the actual TD curve (green solid line) and the corresponding best monotonic fit (black dashed line). (b) Filtered TD obtained by subtracting the exponential best fit from the actual TD curve. (c) The actual spectrum of the trace distance without filtering with a large low frequency component. (d) The power spectrum of the filtered TD, shows two frequency peaks, the one around  $f = 0.02$  (resp.,  $f = 0.25$ ) corresponding to the RTN (resp., position) recurrence component. The importance of this filtering approach is that it allows us to compare the relative strengths of the two sources of non-Markovianity.

$\{\sum_n \Pi_n = \mathbb{I}\}$  and orthogonality  $\{\Pi_n \Pi_{n'} = \delta_{nn'} \Pi_n\}$ . Here,  $\Pi_n = \sum \Pi_c \otimes \Pi_p$ , where  $\Pi_c$  and  $\Pi_p$  denote the projective measurements on the coin and position density matrices  $\rho_c$  and  $\rho_p$ , respectively. Thus,  $\Pi_n$  is the joint projector (tensor product) acting on position space and coin space. It ranges from 1 to  $\text{Dim}(\text{position}) \cdot \text{Dim}(\text{coin})$ .  $\Pi$  is the super-operator acting on the bipartite density operator as a result on the above joint projective measurements. The measurement induced state is given by [57]

$$\Pi(\rho) = \sum_{i,j} (\Pi_c^i \otimes \Pi_p^j) \rho (\Pi_c^i \otimes \Pi_p^j). \quad (28)$$

If the projectors that induces the state  $\Pi(\rho)$  arise from the spectral resolution of the reduced density matrices, *i.e.*,  $\rho_c = \sum_i p_c^i \Pi_c^i$  and  $\rho_p = \sum_j p_p^j \Pi_p^j$ , then the marginal information content remains unchanged; in this sense, the measurement operators are attributed to be least disturbing or optimal. The measure of quantum correlations characterized by MID is the difference between the given density state  $\rho$  and the measurement induced state  $\Pi(\rho)$ ,

$$\mathcal{Q}_{MID} = \mathcal{I}(\rho) - \mathcal{I}(\Pi(\rho)), \quad (29)$$

where  $\mathcal{I}(\cdot)$  is the mutual information, defined as



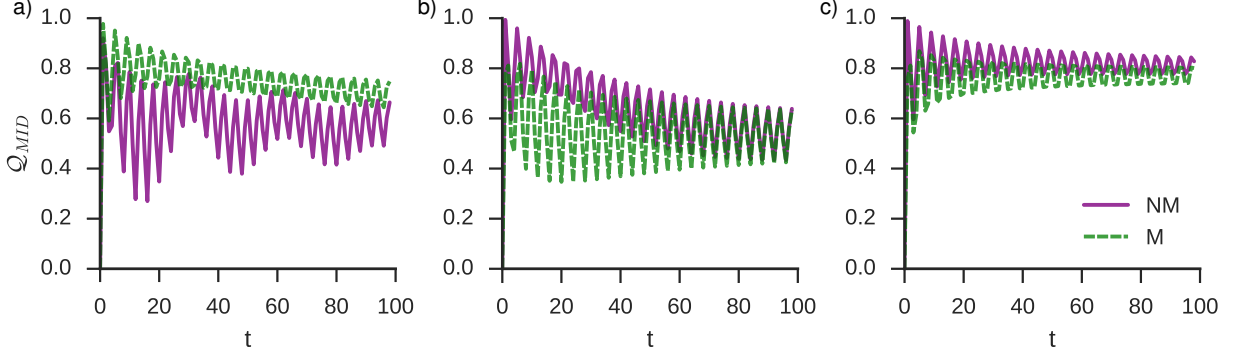


FIG. 6. (Color online) Plot of MID for 100 steps of quantum walk for the initial state  $|\psi(\frac{\pi}{4}, 0)\rangle$  in the presence of RTN, OUN and PLN. The non-Markovian regime is plotted as purple solid line and the Markovian regime is the green dashed line of the respective noise sources. (a) RTN: The interaction between coin and RTN induces oscillations in the non-Markovian regime ( $\gamma = 0.008$ ,  $a = 0.05$ ) indicating the backflow of information from the environment. In the Markovian regime ( $\gamma = 2.0$ ,  $a = 0.05$ ) backflow from RTN is absent and the oscillation is due to position induced non-Markovianity. (b) OUN: In the Non-Markovian region ( $\gamma = 0.01$ ,  $\Gamma = 0.1$ ) unlike RTN no backflow due to the noise is observed, however the decay rate is lesser compared to the Markovian regime ( $\gamma = 2.0$ ,  $a = 0.1$ ). (C). PLN is similar to OUN with no backflow in the non-Markovian regime. The trend observed in the TD and MI cases, is also borne out here.

$$\mathcal{I}(\rho) = S(\rho_C) + S(\rho_P) - S(\rho). \quad (30)$$

## B. Quantum Discord

Next, we use quantum discord (QD) [58, 59] to estimate the difference between the total and classical correlations during the course of quantum walk evolution. QD is defined as the difference between the two natural extensions of classical mutual information to the quantum setting. The first definition of mutual information is given by Eq. (30) and the second definition is the quantum version of conditional entropy which depends on the measurement process. It is defined as follows,

$$\mathcal{J}(\rho_p|\rho_c) = S(\rho_p) - S(\rho_p|\Pi_i^c), \quad (31)$$

where  $S(\rho_p|\Pi_i^c)$  is the quantum conditional entropy, defined with respect to a set of projective measurements  $\{\Pi_i\}$  performed on the coin state  $\rho_c$ . The estimate of QD is then given by,

$$\mathcal{D}(\rho_p|\rho_c) = \mathcal{I}(\rho) - \max_{\Pi_i^c} \mathcal{J}(\rho_p|\rho_c). \quad (32)$$

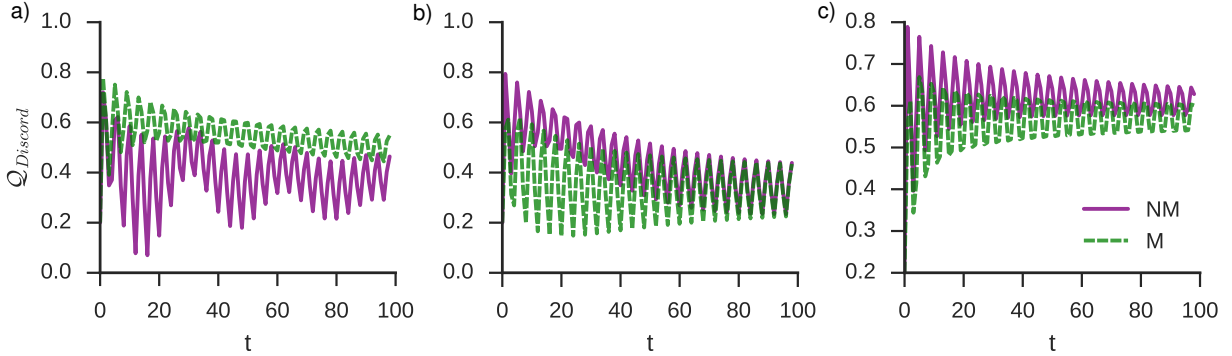


FIG. 7. (Color online) Plot of QD as a function of walk steps  $t$ , under the influence of RTN, OUN and PLN. Note that the noise parameters and the initial state of the particle are same as mentioned for MID. The results are similar to MID for all three noise sources (a) RTN, (b) OUN and (c) PLN, respectively, that drive the coin. QD is strictly a lower bound on the MID between the coin and the position states, due to the optimization performed over the measurement operators. Once again, the trend observed in the TD and MI cases, is borne out here.

QD can be thought of as an optimal version of MID. In MID, the measurement operators that characterize the quantum correlations between the coin and position are given by the corresponding spectral projections and does not involve any optimization. Hence, MID is an operational measure in the sense that computing it is relatively simple. QD on the other hand, optimizes over all possible projectors to compute the correlation between the coin and position states, which makes it computationally intensive.

We have computed both MID and QD numerically for both noiseless and noisy QW, which is shown in Figs. (6) and (7), respectively. In both MID and QD oscillations are observed in the non-Markovian regime of RTN. On the other hand OUN and PLN do not exhibit any oscillations indicating the absence of backflow. Note that the oscillations due to the coin-position interaction vanishes rapidly, because the interaction of the coin with the environment makes the full coin-position system increasingly mixed.

Given that quantum discord is not symmetric, we also considered  $\mathcal{D}(\rho_c|\rho_p)$ , but the pattern of behavior of oscillations in the case of RTN, OUN and PLN, was similar to that seen with  $\mathcal{D}(\rho_p|\rho_c)$ , and this figure is not included here.

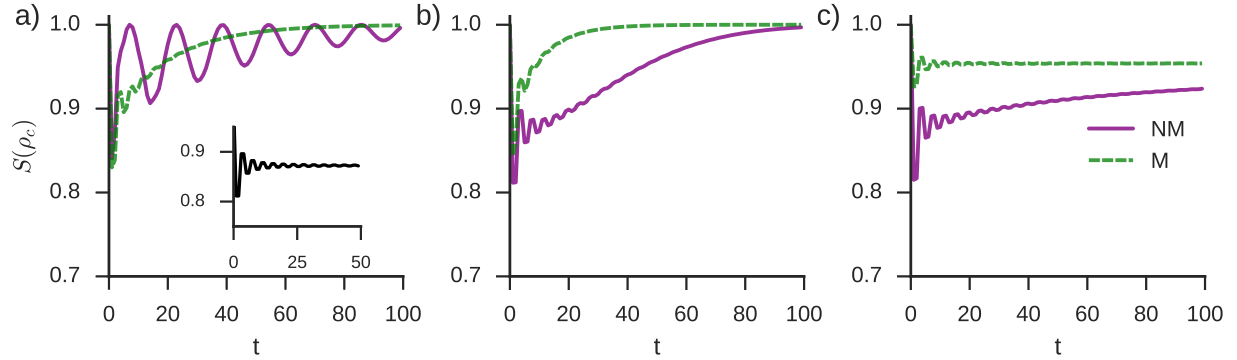


FIG. 8. (Color online) Von-Neumann entropy of the state of the particle under different sources of non-Markovianity. (a) RTN: The backflow effect in the form of oscillations is clearly seen in the non-Markovian regime ( $\gamma = 0.01, a = 0.1$ ). The inset plot is the von-Neumann entropy of noiseless quantum walk. (b) OUN: In both non-Markovian ( $\gamma = 0.01, \Gamma = 1.0$ ) and Markovian regime ( $\gamma = 0.01, \Gamma = 1.0$ ) only the position induced non-Markovianity can be observed. (C) PLN: Similar to OUN, the backflow effects are absent in PLN, the noise parameters are same as OUN.

### C. Quantum purity

Quantum state purity is another interesting quantity that can be used to study the quantumness of quantum walks. Purity, similar to the correlation measures studied previously is a monotone under Markovian evolutions. However under non-Markovian evolutions temporary revivals in purity can be observed in the form of oscillations, this idea has been exploited and studied as a measure of non-Markovianity [60].

Purity can be studied using Von-Neumann entropy  $S(\rho_c) = -\text{Tr}(\rho_c \ln \rho_c)$  where  $\rho_c$  is the reduced state of the particle obtained by tracing out the position degrees of freedom. Note that von-Neumann entropy is maximum for a completely mixed state for which the purity is zero. As noted in the previous discussions, due to the non-Markovianity induced because of the strong entanglement between the particle's internal and external degrees of freedom, the initially pure state of the particle is mapped to a mixed state ( $S \approx 0.875$ ), this is shown in the inset plot in Fig. 8.(a). When the particle is coupled to external source of noise such as RTN, the state of the particle is driven to a maximally mixed state ( $S = 1$ ). We notice that in the non-Markovian regime there is a temporary increase in the purity (decrease in entropy) of the state, this is shown in Fig. 8.(a). In accordance with all other previously observed witnesses of non-Markovianity such as TD, MI, both OUN and PLN does not show any increase in purity and the only source of revival in purity is induced by the position environment.

## VII. CONCLUSION

Quantum non-Markovianity has become an important area of research in the last few years. Here we undertake the task of understanding non-Markovian dynamics, in the context of quantum walks, a familiar “work horse” in quantum information processing. Random telegraph noise (RTN) exhibits backflow, manifesting in terms of oscillations or recurrences in both trace-distance and mutual information as well as not-Complete-positivity of the intermediate map. Non-Markovian noise channels that lack evident backflow are found to be the modified OU noise and the power-law noise (PLN). We develop a power-spectrum technique, that can be adapted to the trace-distance or mutual-information or any other witness methods of backflow, to disambiguate external vs internal sources of backflow. In a QW, these are, typically, the decoherence inducing environment and the position degree of freedom. We also study various facets of quantum correlations in the transition from quantum to classical random walks, under the considered non-Markovian noise models. All of these contribute to our efforts to understand various facets of non-Markovian behavior.

## VIII. ACKNOWLEDGMENTS

SB acknowledges support by the project number 03(1369)/16/EMR-II funded by Council of Scientific and Industrial Research, New Delhi. RS thanks DST-SERB, Govt. of India, for financial support provided through the project EMR/2016/004019. The work of V. J. and F. P. is based upon research supported by the South African Research Chair Initiative of the Department of Science and Technology and National Research Foundation.

- 
- [1] H. P. Breuer and F. Petruccione. *The theory of open quantum systems*. Oxford University Press, (2002).
  - [2] C. M. Chandrashekar, R. Srikanth, and S. Banerjee. *Phys. Rev. A*, **76**, 022316, 2007.
  - [3] S. Banerjee, R. Srikanth, C. M. Chandrashekar, and P. Rungta. *Phys. Rev. A*, **78**, 052316, (2008).
  - [4] S. Banerjee and R. Srikanth. *Phys. Rev. A*, **76**, 062109, (2007).
  - [5] S. Banerjee and R. Ghosh. *J. Phys. A: Math. Theory*, **40**, 13735, (2007).
  - [6] K. W. Murch, U. Vool, D. Zhou, S. J. Weber, S. M. Girvin, and I. Siddiqi. *Phys. Rev. Lett*, **109**, 183602, (2012).
  - [7] S. Omkar, R. Srikanth, and S. Banerjee. *Phys. Rev. A*, **91**, 052309, (2015).
  - [8] S. Shankar, M. Hatridge, Z. Leghtas, K. M. Sliwa, A. Narla, U. Vool, S. M Girvin, L. Frunzio, M. Mirrahimi, and M. H. Devoret. *Nature*, **504**, 419, (2013).

- [9] S. Omkar, R. Srikanth, and S. Banerjee. *Phys. Rev. A*, **91**, 012324, (2015).
- [10] A. Rivas, S. F. Huelga, and M. B. Plenio. *Rep. Prog. Phys.*, **77**, 094001, (2014).
- [11] I. de. Vega and D. Alonso. *Rev. Mod. Phys.*, **89**, 015001, (2017).
- [12] Reichel, J., W. Hansel, P. Hommelhoff, and T. Hänsch, 2001, *Appl. Phys. B* 72, 81.
- [13] Treutlein, P., D. Hunger, S. Camerer, Hänsch, T.W., and J. Reichel, 2007, *Phys. Rev. Lett.* 99, 140403.
- [14] Hunger, D., Camerer, S., Hänsch, T.W., König, D., Kotthaus, J.P., Reichel, J., Treutlein,P, 2010, *Phys. Rev. Lett.* 104, 143002.
- [15] Brouard, S., D. Alonso, and D. Sokolovski, 2011, *Phys. Rev. A* 84, 012114.
- [16] Alonso, D., S. Brouard, and D. Sokolovski, 2014, *Phys. Rev. A* 90, 032106.
- [17] Groblacher, S., A. Trubarov, N. Prigge, G. D. Cole, M. Aspelmeyer, and J. Eisert, 2015, *Nat. Commun.* 6, 7606.
- [18] H. Grabert, P. Schramm, and G. Ludwig. Ingold. *Phys. Rep.*, **168**, 115–207, (1988).
- [19] BL. Hu, J. P. Paz, and Y. Zhang. *Phys. Rev. D*, **47**, 1576, (1993).
- [20] S. Banerjee and R. Ghosh. *Phys. Rev. E*, **67**, 056120, (2003).
- [21] S. Banerjee and R. Ghosh. *Phys. Rev. A*, **62**, 042105, 2000.
- [22] H. P. Breuer, E. M. Laine, and J. Piilo. *Phys. Rev. Lett.*, **103**, 210401, (2009).
- [23] H. P. Breuer, E. M. Laine, J. Piilo, and B. Vacchini. *Rev. Mod. Phys.*, **88**, 021002, (2016).
- [24] A. K. Rajagopal, A. R. Usha Devi, and R. W. Rendell. *Phys. Rev. A*, **82**, 042107, (2010).
- [25] Á. Rivas, S. F. Huelga, and M. B. Plenio. *Phys. Rev. Lett.*, **105**, 050403, (2010).
- [26] D. Chruściński, A. Kossakowski, and Á. Rivas. *Phys. Rev. A*, **83**, 052128, (2011).
- [27] D. Chruściński, Á. Rivas, and W. Storker. *Phys. Rev. Lett.*, **121**, 080407 (2018).
- [28] B. Bylicka, M. Johansson, and A. Acín. *Phys. Rev. Lett.*, **118**, 120501, (2017).
- [29] A. Ambainis, E. Bach, A. Nayak, A. Vishwanath, and J. Watrous. In *Proceedings of the thirty-third annual ACM symposium on Theory of computing*, pages **37–49** (2001).
- [30] C. M. Chandrashekar, S. Banerjee, and R. Srikanth. *Phys. Rev. A*, **81**, 062340, (2010).
- [31] M. Hinarejos, C. Di. Franco, A. Romanelli, and A. Pérez. *Phys. Rev. A*, **89**, 052330, (2014).
- [32] S. Banerjee, N. P. Kumar, R. Srikanth, V. Jagadish, and F. Petruccione. *arXiv:1703.08004*, (2017).
- [33] S. Daffer, K. Wódkiewicz, J. D. Cresser, and J. K. McIver. *Phys. Rev. A*, **70**, 010304, (2004).
- [34] S. O. Rice. *Stochastic Processes in Physics and Chemistry (Elsevier, Amsterdam, 1992)*.
- [35] G. E. Uhlenbeck and L. S. Ornstein. *Phys. Rev.*, **36**, 823, (1930).
- [36] T. Yu and J. H. Eberly. *Opt. Comm.*, **283**, 676–680, (2010).
- [37] W. S. Kendal and B. Jørgensen. *Phys. Rev. E*, **84**, 066120, (2011).
- [38] I. Chakrabarty, S. Banerjee, and N. Siddharth. *Quant. Info and Comp.*, **11**, 541–562, (2011).
- [39] J. Kempe. *Cont. Phys.*, **44**, 307–327, (2003).
- [40] X. Peng and Z. Y. Sheng. *Chin. Phys. B*, **22**, 070302, (2013).
- [41] L. Mazzola, J. Piilo, and S. Maniscalco. *Int. J. Quant. Info*, **9**, 981–991, (2011).
- [42] M. Ali. *Phys. Lett. A*, **378**:2048–2053, 2014.

- [43] J. P. Pinto, G. Karpat, and F. F Fanchini. *Phys. Rev. A*, **88**, 034304, (2013).
- [44] Sandeep. K. Goyal, S. Banerjee, and S. Ghosh. *Phys. Rev. A*, **85**, 012327, (2012).
- [45] E. Paladino, Y. M. Galperin, G. Falci, and B. L. Altshuler. *Rev. Mod. Phys*, **86**, 361, (2014).
- [46] D. W. Leung. *J. Math. Phys*, **44**, 528–533, (2003).
- [47] M. D. Choi. *Linear algebra and its applications*, **10**, 285–290, (1975).
- [48] S. Omkar, R. Srikanth, and S. Banerjee. *Quant. Inf. Proc*, **12**, 3725–3744, (2013).
- [49] S. Omkar, R. Srikanth, and S. Banerjee. *Quant. Inf. Proc*, **14**, 2255–2269, (2015).
- [50] S. Luo, S. Fu, and H. Song. *Phys. Rev. A*, **86**, 044101, (2012).
- [51] E. M. Laine, J. Piilo, and H. P. Breuer. *Phys. Rev. A*, **81**, 062115, (2010).
- [52] E. Novais, A. H. C. Neto, L. Borda, I. Affleck, and G. Zarand. *Phys. Rev. B*, **72**, 014417, (2005).
- [53] S. Banerjee, C. M. Chandrashekar, and A. K. Pati. *Phys. Rev. A*, **87**, 042119, 2013.
- [54] Michael. J. Best and N. Chakravarti. *Math. Prog.*, **47**, 425–439, (1990).
- [55] R. Srikanth, S. Banerjee, and C. M. Chandrashekar. *Phys. Rev. A*, **81**, 062123, (2010).
- [56] B. R. Rao, R. Srikanth, C. M. Chandrashekar, and S. Banerjee. *Phys. Rev. A*, **83**, 064302, (2011).
- [57] S. Luo. *Phys. Rev. A*, **77**, 022301, (2008).
- [58] H. Ollivier and W. H. Zurek. *Phys. Rev. Lett*, **88**, 017901, (2001).
- [59] K. Modi, A. Brodutch, H. Cable, T. Paterek, and V. Vedral. *Rev. Mod. Phys*, **84**, 1655, (2012).
- [60] S. Bhattacharya, A. Misra, C. Mukhopadhyay, and A. K. Pati. *Phys. Rev. A*, **95**, 012122, (2017).